Journal of Contaminant Hydrology 277 (2026) 104864

Contents lists available at ScienceDirect

Journal of Contaminant Hydrology

journal homepage: www.elsevier.com/locate/jconhyd

Microplastics distribution on the beach sediment based on satellite remote sensing: A case study in Bali, Indonesia

Mohd Rashidi Abdull Manap [a,b,*], Muhammad Ibadurrahman bin Imizan [c], Jannik Werner Dams [d], Felipe D. Sepulveda [e], Anna Muratore [f], Lorenza Notargiacomo [f], Fulvio Ferrara [f], Nur Hayatna Mukhni [a]

[a] Department of Chemistry, Faculty of Science, Universiti Putra Malaysia, 43400 Serdang, Selangor, Malaysia
[b] Medical Microspectroscopy Research Group, Department of Experimental Medical Science, Lund University, 22180 Lund, Sweden
[c] School of Biological Sciences, University of Manchester, Oxford Rd, Manchester M13 9PL, United Kingdom
[d] Department of Geography, Rheinische Friedrich-Wilhelms-Universität Bonn, Regina-Pacis-Weg 3, 53113 Bonn, Germany
[e] Departamento de Ingeniería en Minas, Universidad de Antofagasta, Antofagasta 1240000, Chile
[f] National Centre for Water Safety, National Institute of Health (Istituto Superiore di Sanità), Rome, Italy

ARTICLE INFO

Keywords:
ATR-FTIR
Bali
Hydrodynamic modeling
Microplastic
Ocean currents

ABSTRACT

Microplastic (MP) pollution is increasingly recognized as a critical issue in coastal environments, where complex interactions between ocean currents, winds, waves, and human activities govern the transport and deposition of synthetic particles. Although previous studies in Asia have documented MPs accumulation linked to riverine discharge, tourism pressures, and monsoonal circulation, limited work has integrated polymer-level characterization with site-specific hydrodynamic drivers, particularly along the coastlines of Bali. This study addresses this gap by examining how seasonal oceanographic processes influence MPs composition and distribution across three beaches: Keramas Beach (KB), Nyang Nyang Beach (NNB), and Balangan Beach (BB), between January and July 2024. This study provides a baseline, site-specific assessment of microplastic occurrence, polymer composition, and size distribution in three selected beach sediments of Bali, intended to establish reference conditions. Seventeen beach sediments were sampled and processed through dry sieving, microscopy, and attenuated total reflectance-Fourier transform infrared (ATR-FTIR) spectroscopy to identify particle sizes, morphologies, and polymer types. Hydrodynamic conditions were reconstructed using satellite-derived datasets from the Copernicus Marine Environment Monitoring Service (CMEMS) and the Copernicus Atmosphere Monitoring Service (CAMS), alongside estimates of riverine plastic discharge. A total of 10 MP particles (<5 mm) were identified, with polystyrene (PS) as the dominant polymer, followed by polypropylene (PP), polyvinyl alcohol (PVA), polymethyl methacrylate (PMMA), and three copolymers. MPs occurred primarily as fragments within the 2.5–5 mm range. The average MP concentrations were 2.54 ± 2.30, 2.04 ± 2.49, and 0.61 ± 1.37 MPs/kg dry weight (dw) at KB, NNB, and BB, respectively, following the order KB > NNB > BB. Spatial variability corresponded closely with hydrodynamic patterns: KB exhibited the highest MP concentration due to onshore winds and southwestward currents from the Lombok Strait; BB showed low retention driven by offshore wind stress and weak currents; and NNB displayed intermediate accumulation influenced by longshore drift and moderate river inputs. These findings highlight the value of integrating spectroscopic analysis with remote-sensing hydrodynamics to explain mechanisms of MP deposition, offering a strengthened basis for targeted monitoring, predictive modeling, and coastal pollution management in Bali and neighboring islands.

1. Introduction

Ocean current plays a central role in controlling the transport, redistribution, and fate of marine pollutants, including microplastics (MPs), polycyclic aromatic hydrocarbons (PAHs), and persistent organic pollutants (POPs). Due to their persistence and buoyancy, MPs can be

* Corresponding author at: Department of Chemistry, Faculty of Science, Universiti Putra Malaysia, 43400 Serdang, Selangor, Malaysia; Medical Microspectroscopy Research Group, Department of Experimental Medical Science, Lund University, 22180 Lund, Sweden.
E-mail addresses: rashidichemistry@upm.edu.my, rashidi.manap@med.lu.se (M.R.A. Manap).

https://doi.org/10.1016/j.jconhyd.2026.104864
Received 30 September 2025; Received in revised form 14 January 2026; Accepted 19 January 2026
Available online 20 January 2026

transported over long distances and act as vectors for chemical contaminants, amplifying ecological exposure across marine food webs (Li et al., 2022; Kumar et al., 2024; Ho et al., 2025).

MP pollution is particularly pronounced in intensively used coastal regions with strong land-sea connectivity, where riverine discharge, tourism-related activities, and inadequate waste management substantially increase plastic inputs to the marine environment (Borah et al., 2024). Rivers serve as major transport pathways and exposure zones, where MPs interact with dissolved and particulate-bound pollutants before entering coastal waters. In freshwater and estuarine systems, MPs can adsorb PAHs, heavy metals, pesticides, and other toxic compounds, increasing bioavailability to benthic organisms and posing risks to ecosystem and human health through trophic transfer. Beach sediments, therefore, act as sinks and temporary reservoirs for MPs, integrating inputs over time and reflecting local transport dynamics. Across Asia, MP distributions reflect the combined influence of land-based sources, riverine discharge, and offshore circulation, with polyethylene (PE) and polypropylene (PP) consistently reported as dominant polymers (Ajay et al., 2025; Thibault et al., 2025).

At the coastal scale, MP transport and deposition are governed by interactions between particle-specific properties and hydrodynamic processes. Particle density, size and shape influence responses to wind, waves, currents, and tidal dynamics in the nearshore zone (Kumar et al., 2025). While low-density polymers commonly follow surface circulation, denser polymers are more susceptible to biofouling-induced sinking; however, buoyant MPs are frequently observed in bottom sediments due to vertical mixing and resuspension, indicating that polymer density alone does not determine MP fate (Jiang et al., 2024).

Despite advances in hydrodynamic modeling, particle-tracking simulations, and satellite remote sensing, uncertainties in particle behavior and limited resolution of nearshore processes continue to constrain predictions of beach-level MP deposition, particularly in tropical coastal systems with strong seasonality and complex shoreline morphology (Cai et al., 2023; Ma et al., 2023; Karimi et al., 2024; Raja et al., 2024; Mali et al., 2025).

Within Southeast Asia, MP transport across the Indonesian archipelago is shaped by riverine discharge, monsoonal wind systems, and regional ocean circulation. Modeling studies indicate that MPs released from Indonesian rivers tend to accumulate near major islands due to circulation pathways and sinking behavior (Iskandar et al., 2024; Nakano et al., 2025). Elevated MP fluxes have been reported in highly urbanized river systems such as Jakarta, while subsurface accumulation linked to density stratification and temperature gradients has been observed within the Indonesian Throughflow (ITF) (Manullang et al., 2024). Regional surveys further reveal pronounced spatial variability across the archipelago, with higher subsurface MP concentrations in eastern Indonesian waters compared to northern Java, underscoring the role of regional hydrography in shaping MP distributions (Riani and Cordova, 2022).

Bali represents a dynamic but understudied system within this regional context. Its oceanographic setting is governed by monsoonal wind reversals, the ITF, and large-scale climate oscillations such as the Indian Ocean Dipole (IOD) and El Niño-Southern Oscillation (ENSO), which collectivley regulate surface circulation, mixing intensity, and seasonal transport pathways (Wijaya et al., 2020; Suntoyo and Wahyudi, 2021; Adhinugraha et al., 2023; Alkoiri et al., 2024; Widyananto et al., 2024). Seasonal transitions between the Southwest and Northeast monsoons are therefore expected to exert strong control over MP transport and beach-level deposition along Bali's coastlines (Wang et al., 2021; Hee et al., 2023; Kannankai and Devipriya, 2024; Carvalho et al., 2025; Prajapati et al., 2025).

Despite Bali's ecological and socio-economic significance, few studies have integrated satellite-derived oceanographic data with Geographic Information System (GIS)-based spatial analysis to examine MP transport and deposition at the beach scale. In this context, we hypothesized that beaches influenced by stronger onshore currents and winds would exhibit higher MP retention, whereas sites exposed to weaker currents and offshore wind components would experience enhanced dispersion and lower accumulation. We further hypothesized that seasonal current reversals and regional circulation pathways facilitate both riverine and long-range MP transport from northern Bali, Java, and the Lombok Strait, resulting in distinct accumulation regimes across eastern, central, and western coastlines.

This study addresses these hypotheses by combining field-based MP inventories with satellite-derived ocean current and wind data to evaluate spatial and seasonal deposition patterns at three representative beaches in Bali—Keramas Beach (KB), Nyang Nyang Beach (NNB), and Balangan Beach (BB). Physical characteristics of MPs in beach sediments are assessed alongside ocean circulation and riverine plastic discharge between January and July 2024, using datasets from the Copernicus Marine Environment Monitoring Service (CMEMS) and the Copernicus Atmosphere Monitoring Service (CAMS). By linking polymer-level characterization with hydrodynamic drivers, this work provides mechanistic insight into MP transport in a monsoon-dominated island system and supports monitoring and mitigation strategies in Bali and comparable Southeast Asian coastal environments.

2. Methods

2.1. Sampling and characterization of MPs

MP samples were collected in early August 2024 from three beaches in Bali, Indonesia: KB (a tourist hotspot), BB, and NNB (a less-visited beach) without a field blank (Manap, 2025). Seventeen sampling points, with two replicate samples each, were selected across the sites: at distances ranging from 100 to 130 m on KB, 70 to 110 m on BB, and 90 to 215 m on NNB. Due to the field constraint of strong ocean waves during the field sampling, a total of 251.33 cm^3 of beach sediments was dry-sieved using cylindrical stainless steel sieves with mesh sizes of 5.60 mm, 710 μm, and 212 μm to separate the particles by size in this exploratory work. Residues on each sieve were re-examined, thereby maximizing the recovery of MPs. Best-practice guidance in beach sediment sampling often employs a series of sieves with mm-sized openings to retain MP samples in each sieve before microscopic and characterization (Gimiliani et al., 2020). The detection limit of the current work is larger than 212 μm, and smaller particles ($<$212 μm) are not reported due to limitations in detection methodology, rather than the absence of MP contamination. A total of 44 particles were recovered; 8 particles exceeding 5 mm were excluded, while 36 particles under 5 mm were retained for further analysis (Manap, 2024a). The retained particles were transferred into labeled Eppendorf tubes. Each particle was mounted on a glass slide and examined under an Olympus CX33a transmitted light microscope equipped with a digital camera and connected to a monitor. A 4× objective lens was used for size calibration with a ruler, and particle dimensions were recorded based on the longest axis of each particle. Fourier transform infrared (FTIR) spectra were acquired using a Shimadzu IRAffinity-1S spectrophotometer with an attenuated total reflectance (ATR) accessory. Measurements were conducted in the 4000–370 cm^{-1} range at a resolution of 4 cm^{-1}, with an average of 32 scans per spectrum (Manap, 2024b). The instrument operated in % transmittance mode with Happ-Genzel apodization and a mirror speed of 2.8. No spectral preprocessing was applied prior to library matching.

As part of the Quality Assurance and Quality Control (QA/QC) process, the ATR crystal (diamond/ZnSe) was cleaned between measurements to prevent contamination. Background scans were performed to remove the spectral contributions from the spectrometer and the laboratory air. Airborne contamination was controlled by maintaining a clean laboratory, handling samples and conducting microscopic analysis from individual vials, and wearing appropriate clothing during both field and laboratory activities. Density separation was applied as the primary extraction method based on buoyancy differences between plastic polymers and mineral particles, with only filtered seawater used for rinsing and apparatus cleaning to prevent secondary contamination.

During the density separation process, the seawater was first inspected to confirm the absence of visible particles. Due to airline restrictions to Indonesia, sufficient quantities of sodium iodide required for laboratory-based density separation could not be delivered to Bali, and the sand samples could not be transported back to the laboratory in Malaysia. Therefore, only seawater was used as the separation medium for the sand and MPs. To avoid sample misclassification, each isolated particle was stored in an individual microtube before IR measurement in Thailand.

2.2. Remote sensing and GIS tools

Remote sensing through satellite observation represents one of the two primary approaches for collecting oceanographic data, complementing traditional in situ measurements. This method is crucial for evaluating the effects of climate change and anthropogenic activities on marine environments. Although in situ validation would enhance the reliability of remote sensing analyses, such validation is currently constrained by the limited availability of observational datasets for the study area. At present, there are no active buoys, gliders, or other oceanographic monitoring systems operating near Bali Island, and no public databases provide in situ measurements of current velocity, wave height, or wind fields in this region. Consequently, the use of satellite-derived products constitutes the most viable and comprehensive approach for obtaining consistent hydrodynamic and atmospheric data across relevant spatial and temporal scales.

Despite certain limitations, such as coarse spatial resolution and potential atmospheric attenuation, satellite observations offer global coverage and enable the monitoring of key oceanographic parameters, including surface currents, winds, and wind waves. Ocean current velocity is derived indirectly, reconstructed from sea surface height (SSH) measured by satellite altimeters, in combination with surface wind and sea surface temperature (SST) fields incorporated into physical circulation models (Dohan and Maximenko, 2010). Wind parameters are obtained directly from satellite-based instruments such as scatterometers and Synthetic Aperture Radar (SAR) sensors (Yang et al., 2011). Altimeters and SAR sensors also provide wind waves height and direction, respectively.

CMEMS platform (MyOcean Pro, https://data.marine.copernicus.eu/viewer/expert) offers the capability to download global current data archived in a database called Global Ocean Physics Analysis and Forecast (CMEMS, 2024a) for any specified area and time intervals (monthly average, daily average, 6-h average). Similarly, another database called Global Ocean Waves Analysis and Forecast (CMEMS, 2024b) allows the download of wind waves direction, magnitude, and height for each day at a three-hour time interval. CAMS offers the same possibility for wind, providing access to data from the CAMS Global Greenhouse Gas Forecasts database (CAMS, 2024a).

The portals offer access to digital files that can be downloaded in the National Cartographic Standard (NCS) format. These files are presented as raster files, which are composed of pixels. Raster files can be imported into a GIS-type program, such as QGIS (version 3.34.9), an open-source program that enables the extraction of vector information from each pixel and maps the locations of sampling sites. A series of tools has been developed to facilitate this process, including the VectorFieldCalc plugin v1.5.4 and the Point Sampling Tools v0.5.4. These tools extract vector information (magnitude and orientation) from each pixel and place it within a variable number of chosen points. These points are transformed into arrows, with the intensity proportional to the speed of the current or wind, and the arrow's direction indicating the prevailing current or wind during the selected time period. Current data were downloaded as the monthly average. The CAMS facilitates the download of wind data at varying altitudes on a daily and hourly basis. The file was imported into QGIS, where the preferred level of elaboration between mlev (model level) and plev (pressure level) was selected. The methodology employed involved utilizing the mlev function, in line with established protocols for current analysis. The vector information (magnitude and orientation) in the raster file was integrated into the points, as previously done for currents, resulting in the appearance of arrows. Wind data was downloaded as the 12:00 hourly average at sea level pressure (1000 hPa).

A primary limitation of this approach is the native satellite resolution, which can result in data gaps in nearshore regions. In particular, the CMEMS Global Ocean Physics Analysis and Forecast and the Global Ocean Waves Analysis and Forecast datasets have a horizontal resolution of 1/12° (~0.083°), corresponding to approximately 8 km, while the CAMS Global Greenhouse Gas Forecasts dataset provides a coarser resolution of about 40 km. Additionally, the models employed to reconstruct currents, waves, and wind intensity are subject to a degree of uncertainty. According to the Quality Information Document (QID) of the Global Ocean Physics Analysis and Forecast database, there is an underestimation of the currents compared to in situ measurements carried out using drifters. The underestimation is 20% for strong currents and 60% for weak currents. For waves, the QID of the Global Ocean Waves Analysis and Forecast database reports an average bias of 2 cm and a scatter index of 13.8% on wave height. For winds, the European Centre for Medium Range Weather Forecasts Technical Memo n° 918 (Evaluation of ECMWF forecasts) reports a RMSE of 1–3 m/s for the wind speed. These constraints may reduce the accuracy of current and wind estimates close to the coastline; however, satellite-derived products remain the most reliable and spatially consistent data source currently available for hydrodynamic assessment in Bali Island.

3. Results and discussion

3.1. Characterization of MPs synthetic polymers

This study was designed as an exploratory baseline assessment of MPs occurrence in beach sediments, with an emphasis on spatial patterns and hydrodynamic controls rather than exhaustive quantification of MPs. Given the field constraints associated with coastal sampling in a tropical environment, the analytical strategy prioritized the recovery and confident identification of the larger MP size fraction (>212 μm) using dry sieving, visual screening, and ATR-FTIR confirmation. Consequently, the reported MP concentrations represent an estimate of the detectable size range and should be interpreted as indicative of relative spatial variability among beaches rather than absolute concentrations. MPs were detected in eight out of the seventeen sampling sites, with a total of ten particles (Tables S2 & S3). The MPs differed in their material composition, with polystyrene (PS) being the most frequently identified polymer. Other common synthetic polymers, including PP, polyvinyl alcohol (PVA), and polymethyl methacrylate (PMMA, or commercially known as acrylic), were also detected. Interestingly, three particles were identified as copolymers.

The size distribution of the MPs was dominated by particles in the 2.5–5 mm range, followed by those in the 1–2.5 mm range. Fragment-type MPs constituted the majority (8 out of 10 particles), whereas foam- and bead-type MPs occurred less frequently. In terms of color, green and white particles were predominant, while purple, yellow, and red particles appeared less abundantly. The concentrations of MPs (per kilogram of dry sand) of all sampling sites on each beach are shown in Table 1. Among the studied sites in Bali, KB exhibited the highest MP concentration, with a mean of 2.54 ± 2.30 MPs/kg dry weight (dw), followed by NNB (2.04 ± 2.49 MPs/kg dw). The lowest concentration was recorded at BB, averaging 0.61 ± 1.37 MPs/kg dw. Notably, there is low variability in MP abundance among sites within each beach, with the observed pattern typically consisting of one to two particles in the sediment samples where MPs were present. Consequently, low deviations in MPs abundance are observed on these beaches.

The concentrations of MPs across sites from the three beaches in this

Table 1
MP concentrations for each beach with mean ± standard deviation.

Beach/ site	Total MPs	MP concentration per site (MPs/kg dw)	MP concentration per beach (MPs/kg dw)		
			Mean	Range	SD
KB/01	1	3.05	2.54	0.00–6.11	2.30
KB/02	1	3.05			
KB/03	2	6.11			
KB/04	1	3.05			
KB/05	0	0.00			
KB/06	0	0.00			
BB/01	1	3.05	0.61	0.00–3.05	1.37
BB/02	0	0.00			
BB/03	0	0.00			
BB/04	0	0.00			
BB/05	0	0.00			
NNB/01	0	0.00	2.04	0.00–6.11	2.49
NNB/02	0	0.00			
NNB/03	1	3.05			
NNB/04	1	3.05			
NNB/05	2	6.11			
NNB/06	0	0.00			

SD – standard deviation.

study were substantially lower than those reported in previous investigations of MP contamination in nearshore sediments from Bali and nearby islands (Table 2). In another part of Bali Island, sediment MP concentrations have been reported to reach approximately 90 MPs/kg dw. A study documented an average of 90.7 ± 59.1 MPs/kg dw in Badung (Mauludy et al., 2019). Similarly, a 2024 study reported comparable levels in Benoa Bay, with concentrations ranging from 9.51 to 90.60 MPs/kg dw (Suteja et al., 2024). Sediments from Gili Trawangan in neighboring Lombok Island exhibited relatively low MP concentrations, ranging from 6.00 ± 8.49 to 22.00 ± 30.84 MPs/kg dw (Chairunnisa et al., 2025); however, these values were slightly higher than the concentrations measured in this study.

Much higher levels have been reported across Java Island. In the East Canal Flood (ECF) and Babon River estuaries of Central Java, MP pollution reached an average of 22,710 MPs/kg dw (Tjahjono et al., 2024). In Banten Bay and Jakarta Bay, concentrations exceeded 100 MPs/kg dw, with reported values ranging from 182 ± 82.97 to 346 ± 144.24 MPs/kg in Banten Bay and 166.8 MPs/kg in Jakarta Bay (Takarina et al., 2022; Noor et al., 2025). Along the eastern coast of Java, which is geographically close to Bali, four beaches recorded concentrations between 54.7 ± 48.6 and 103.3 ± 4.7 MPs/kg dw (Yona et al., 2023), while sediments near Bama Resort at Baluran National Park averaged 116.41 ± 80.78 MPs/kg dw (Asadi et al., 2019).

Table 2
Comparison of MP concentration from nearshore sediments between this study and neighboring regions.

Reference	Location	Concentration (MPs/kg dw)
Curren and Yew Leong (2023)	Coastal regions along Johor & Singapore Straits, Singapore	31.1 to 59.9 (Johor Strait) 9.2 (Singapore Strait)
Zahari et al. (2023)	Tanjung Aru Beach & UMS ODEC Beach, Kota Kinabalu, Sabah, Malaysia	56 to 352 (Tanjung Aru Beach) 17 to 34 (UMS ODEC Beach)
Tjahjono et al. (2024)	East Canal Flood & Babon River, Semarang, Indonesia	22,710
Noor et al. (2025)	Banten Bay, Indonesia	182 ± 82.97 to 346 ± 144.24
Takarina et al. (2022)	Jakarta Bay, Indonesia	166.8
Yona et al. (2023)	Eastern Java Island, Indonesia	54.7 ± 48.6 to 103.3 ± 4.7
Asadi et al. (2019)	Bama Resort, Baluran National Park, Indonesia	116.41 ± 80.78
Chairunnisa et al. (2025)	Gili Trawangan, Lombok, Indonesia	6.00 ± 8.49 to 22.00 ± 30.84
Suteja et al. (2024)	Benoa Bay, Bali, Indonesia	9.51 to 90.60
Mauludy et al. (2019)	Coastal beaches in Badung, Bali, Indonesia	90.7 ± 59.1
This study	Keramas Beach (KB), Balangan Beach (BB), Nyang Nyang Beach (NNB), Bali, Indonesia	0.61 ± 1.37 to 2.54 ± 2.30

UMS – Universiti Malaysia Sabah; ODEC – Outdoor Development Center.

Beyond Indonesia, a study in Singapore reported MP concentrations ranging from 9.2 to 59.9 MPs/kg dw along the coastal regions of the Johor Strait-Singapore Strait (Curren and Yew Leong, 2023), which remain higher than the values observed here. Further north, beaches in Sabah, Malaysia, exhibited even greater concentration, with Tanjung Aru Beach (857 MPs/kg dw total MP concentration) far exceeding both UMS ODEC (Universiti Malaysia Sabah Outdoor Development Center) Beach (160 MPs/kg dw) and the concentrations measured in this study (Zahari et al., 2023). Overall, findings from regional studies consistently show that the MP levels detected here are among the lower concentrations reported in regional studies. A similar observation of a relatively low proportion of particles being classified as microplastics has been reported in Auckland, New Zealand, with only 22% of the recovered particles confirmed as microplastics (Bridson et al., 2020).

Figs. 1 and 2 show an approximation of the sampling points in photographs of two of the most polluted beaches, showing the types of MPs, colors, and the linear trend of each of the colors. The results are visually clear: the sampling points with the highest presence of these MPs are concentrated in the vicinity of tourist facilities and near the beach.

Meanwhile, Fig. 3 illustrates the distribution of MP fragments on Bali beaches. Overall, the findings emphasize the influence of land-based human activities on the distribution of coastal MPs, highlighting spatial variation in MP contamination, with stronger pollution signatures observed in more urbanized or touristic beaches.

FTIR spectroscopy was used to confirm the chemical identity of MPs recovered from the beach sediments, with a minimum hit quality of 627. Previous microplastic work has demonstrated that a minimum spectral matching score of 60% with a reference library provides reliable confirmation of polymer identity, particularly for smaller-sized microplastics where spectral distortion and surface weathering are more pronounced. A matching score exceeding this threshold has been shown to adequately validate polymer classification while minimizing false-positive assignments (Rathore et al., 2023). Therefore, the threshold values applied in this work are consistent and sufficient for confident microplastic identification.

Fig. 4 displays the representative FTIR spectrum of an MP sample identified as PS. The identification was validated using a spectral library match with a hit quality score as guidance, spectral confirmation by an expert spectroscopist, and cross-checking against the Open Specy online database. Among these MPs, PS was the most frequently detected polymer, particularly in BB and NNB. The acquired FTIR spectrum of PS exhibits several prominent C—H stretching vibrations between 3024 and 2920 cm^{-1}. In addition, IR absorption peaks attributed to C=C–H bending of the aromatic is observed at approximately 1450 cm^{-1}. Notably, aromatic C=C stretching vibrations appear at 1601 cm^{-1}, further confirming the presence of PS. On top of these PS signals, the ATR-FTIR spectrum of the PS samples obtained from the beach sediments yields several major new features in the 3800–3100 cm^{-1} (O—H stretching) and 1100–900 cm^{-1} (C–O/C–C stretching) regions. Despite small peak shifting, the spectral features of the samples are in very good agreement with reference data for a pure PS sample, with a known density of 1.05 g/cm^3 (Aouissi et al., 2023). The clear alignment of spectral features with known reference materials strengthens the confidence in polymer identification and supports the reliability of FTIR as a non-destructive tool in environmental MP studies.

Figs. S1-S3 show the comparison between the raw FTIR spectra of

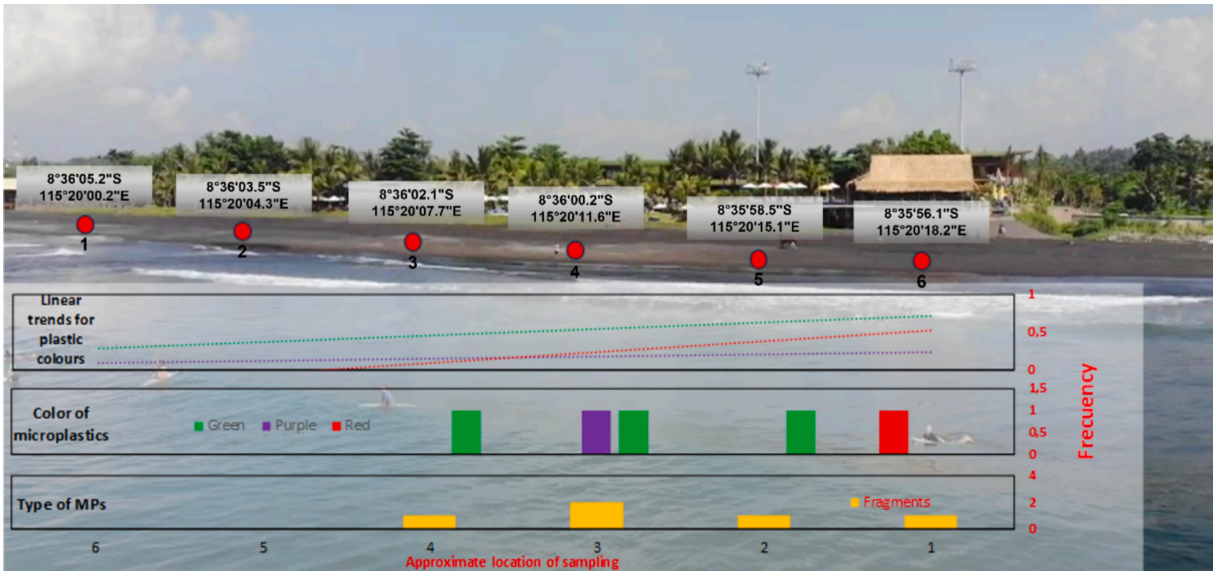

Fig. 1. Approximate sampling analysis for KB, illustrating the frequency of MP fragments and the linear trends of plastic colors across the sampling sites.

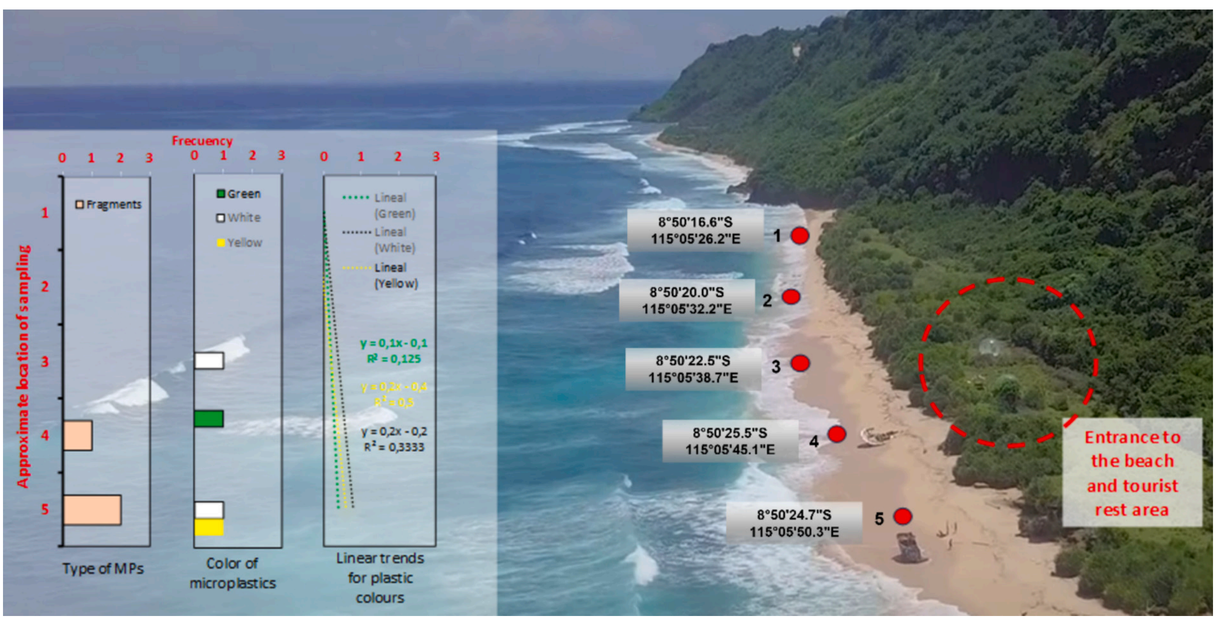

Fig. 2. Approximate sampling analysis for NNB, illustrating the frequency of MP fragments and the linear trends of plastic colors across the sampling sites.

three samples from this study and their corresponding spectral library match results (Manap, 2024b). While the quality of the acquired spectra varied, most exhibited medium to strong signal intensities.

3.2. Study on ocean currents, wind, and wind waves

A study of ocean currents, winds, and wind waves should be considered, as these factors may influence the distribution of MPs in beach or ocean environments. The study was conducted in accordance with the methods outlined in Section 2.2. The aforementioned methods were further augmented by incorporating the database from Meijer et al. (Meijer et al., 2021a). The database is available on Figshare (Meijer et al., 2021b), online (TheOceanCleanup, 2017), and aggregates data on plastic inputs (in kg/km^2/year) from the world's major rivers. Data were aggregated into three categories (Fig. 5): green (0.50 kg/km^2/year), yellow (3.80 kg/km^2/year), and red (over 3.80 kg/km^2/year). This configuration enabled the immediate identification of the most impactful sources.

In order to gain insight into the currents that could potentially transport particles to the sampled beaches, a methodology was employed in which files were downloaded as described in methodologies for the area of the world around the island of Bali and for the months from January 2024 to July 2024 This approach enabled comprehensive coverage of the entire time pre-sampling time interval and facilitated a nuanced understanding of the changing currents.

Fig. 5 illustrates a comprehensive examination of current trends in the region surrounding Bali Island from January to July 2024. Fig. 5G(a) provides a detailed view of the area near the coastal zones. During the winter months of January, February, and March, the currents, as represented by the monthly average direction, exhibit a consistent movement pattern. At the western beaches (NNB and BB), these currents originate from Java Island and move eastwards. In contrast, at KB Beach in the east, the prevailing current moves in a north-south direction during this period. Although the trend at KB is less pronounced, a

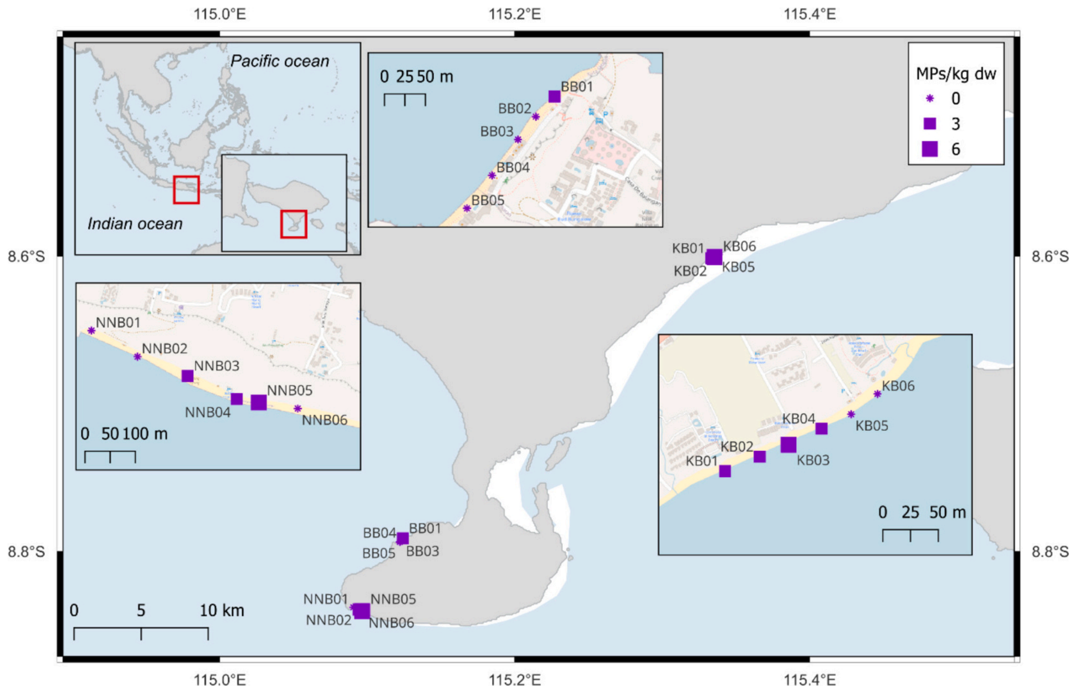

Fig. 3. MP fragment distribution on Bali beaches in MPs/kg dw.

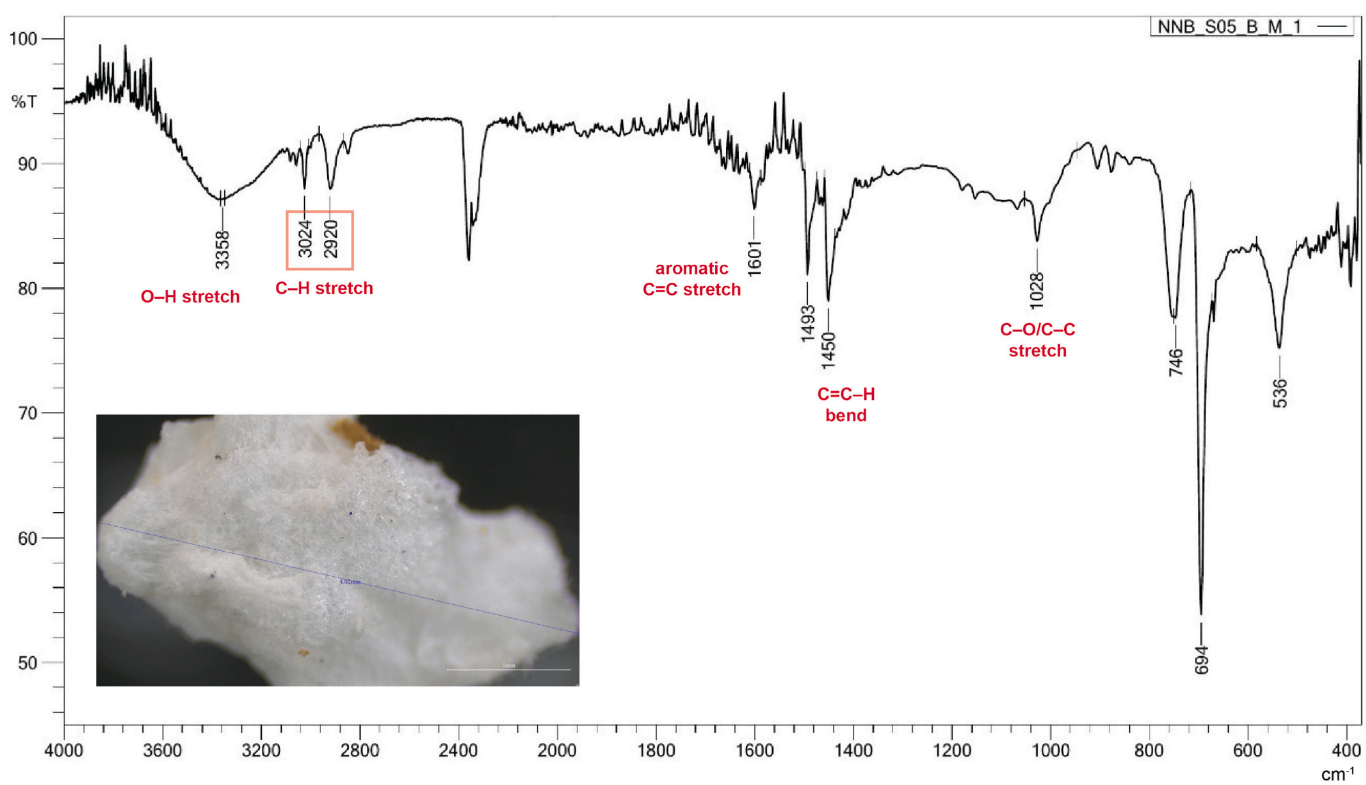

Fig. 4. ATR-FTIR spectrum of a sample identified as MP of PS.

southward current movement is still discernible along this coastline. Since April, a seasonal change has begun to manifest. In the western region of Bali Island, including NNB, the currents migrate northwards. Meanwhile, KB Beach exhibits a more intense and persistent north-south current, similar in direction to that observed in winter, but with increased magnitude. The only significant change during the summer months occurs again in the western part of the island. Here, the currents reverse direction, moving from Bali toward Java, as illustrated in Fig. 5G. These western beaches may receive plastics transported from the southern coast of Java. As a result of prevailing current directions, the currents that flow from the direction of Java toward western Bali beaches suggest potential transport pathways of MPs. During the spring, the current flow from Java decreases in intensity and gradually reverses direction. Consequently, the anthropogenic impact from the northern

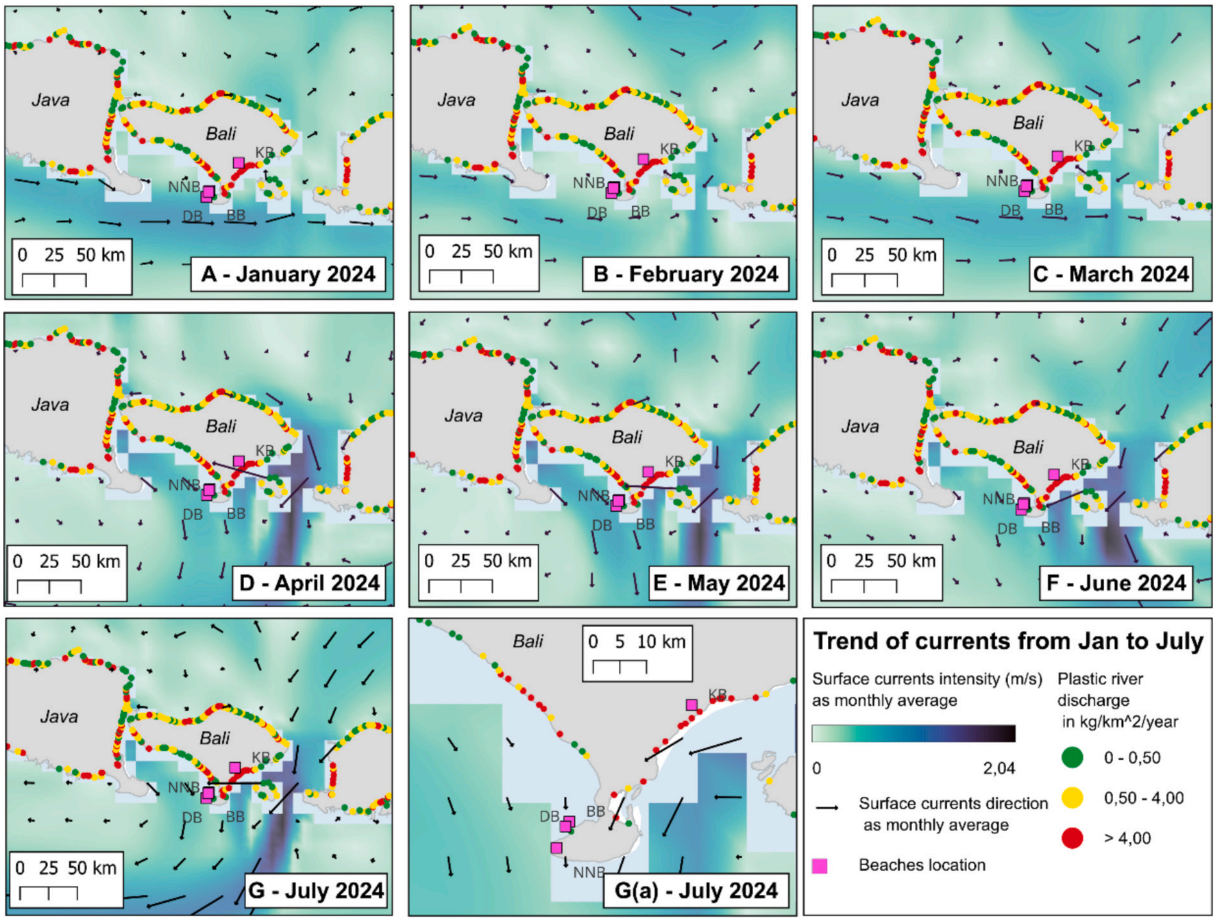

Fig. 5. Surface current trends from January to July 2024 (A to G) and sources of impact (river discharge in kg/km^2/year). Figure G(a) represents a zoom of G to better visualize the beach location on Bali Island. Currents are represented as monthly time averages, with arrows indicating both direction and magnitude; the length of the arrows is proportional to current intensity. Magnitude is also represented by a color scale. In areas near the coast, current values are missing due to the satellite resolution of the currents database (about 8 km). Current data comes from the Global Ocean Physics Analysis and Forecast by CMEMS (CMEMS, 2024a) has a horizontal resolution of 1/12° (~0.083°), corresponding to approximately 8 km. In this database, surface currents of the mid latitudes are underestimated on average with respect to in situ measurements of drifting buoys. The underestimation ranges from 20% in strong currents to 60% in weak currents. Plastic river discharge is from Meijer et al. (Meijer et al., 2021a).

region of the island of Bali may prevail on the beaches situated to the west. During the summer months, there is a complete reversal of the flow. The eastern beach is influenced by flows from the Lombok Strait during the winter. During spring and summer, the beach is affected by an increasing flow from the Lombok Strait. However, the beach itself is an area where rivers have a significant local impact.

Quantitative and graphical representations of the main oceanographic parameters considered in this study for the three sampled beaches are shown in Table 3 and Figs. 7 and 8.

The table presents the predominant direction, period, and height of wind waves, as well as the direction and magnitude of surface currents and the corresponding components of the wind vector during the sampling days (3 and 5 August 2024). These parameters enable a direct comparison between the eastern (KB), central (NNB), and western (BB) coasts of Bali. The interplay of these factors exerts a profound influence on the retention, redistribution, or export of floating MP particles along each coastline.

Fig. 6 presents a comprehensive depiction of the currents (as the monthly average in July 2024 and as the daily average of the sampling days, indicated by red, blue, and green arrows) that arrived on the beaches, with the sampling stations highlighted. These currents remain constant within the selected time intervals. It should be noted that the absence of arrows in KB is due to the fact that the satellite resolution does not cover areas close to land; however, the movement of the currents can be deduced from those in adjacent areas. Magnitude in m/s shows that in the KB area, currents have a velocity of around 1.2 m/s, in

Table 3
Wind wave direction, period, and height, currents, and wind direction and magnitude on 3 and 5 August 2024. Direction is expressed as degrees, considering the originating point for waves and the direction point for currents and wind. Magnitude is expressed in m/s and height in m.

Beach	Wind wave direction (°)	Wind wave period (s)	Wind wave height (m)	Current direction (°)	Current magnitude (m/s)	Wind direction (°)	Wind magnitude (m/s)
KB	19.7 151.7 252.2	1.2	0	240.66	1.12	276.56	2.56
BB	126.2	1.8	0.34	186.65	0.31	276.56	4.81
NNB	126.2	2.0	0.21	183.39	0.27	276.56	4.81

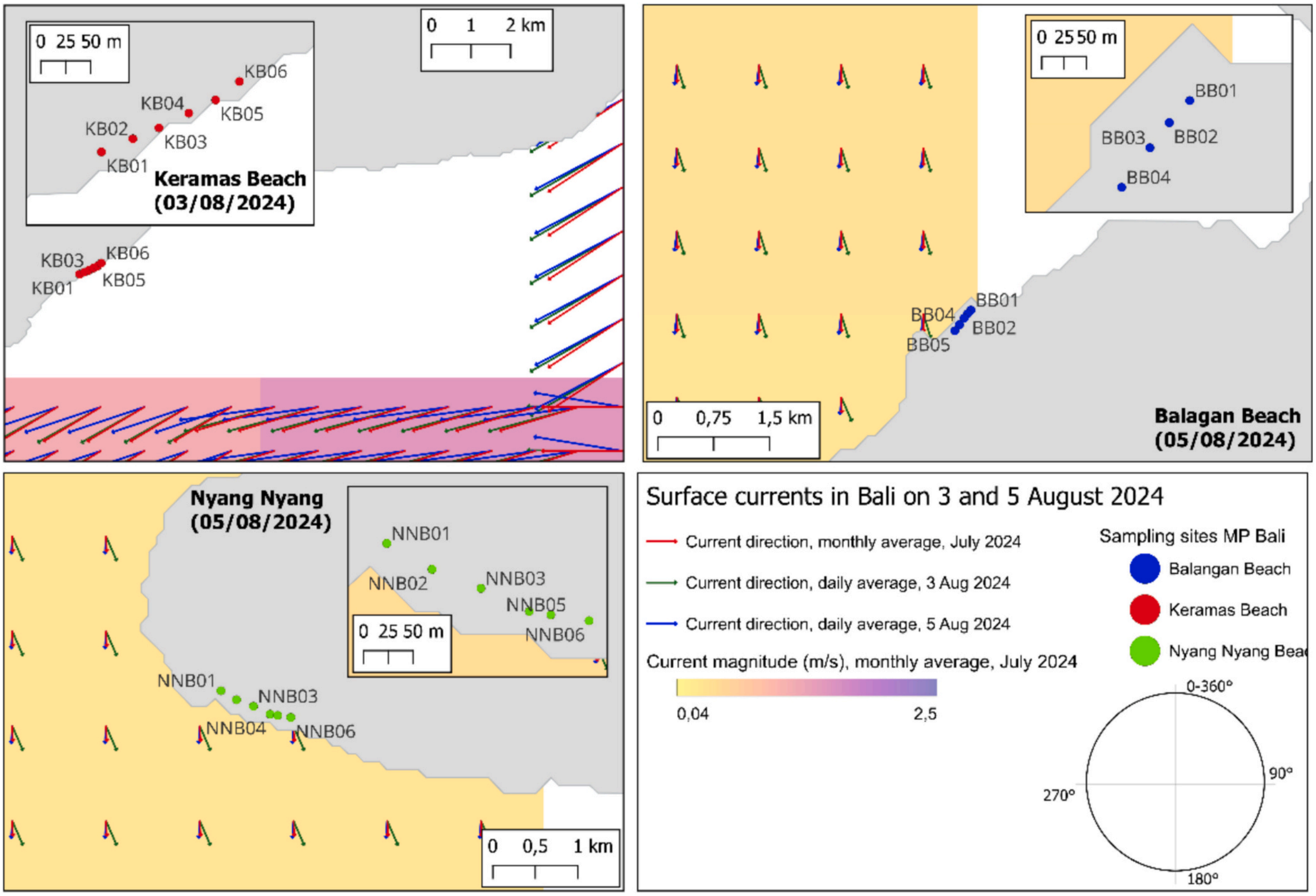

Fig. 6. Surface currents on the individual beaches. Detailed sampling sites are highlighted, and the current direction and magnitude (as arrow length) are represented as monthly time averages for July 2024 and daily averages for 3 and 5 August 2024. The July 2024 current magnitude is also represented in scaled colors: magnitude 0 (white) is due to missing data resulting from satellite resolution of the currents database, Global Ocean Physics Analysis and Forecast by CMEMS (CMEMS, 2024a): horizontal resolution of 1/12° (~0.083°), corresponding to approximately 8 km. In this database, surface currents in the mid latitudes are, on average, underestimated relative to in situ measurements from drifting buoys. The underestimation ranges from 20% in strong currents to 60% in weak currents. Note that for current, the direction in degrees indicates where the current is flowing.

the south area (NNB and BB), velocities are much lower, around <1 m/s, as summarized in Table 3.

As previously mentioned, CAMS allows users to download wind data at different altitudes on a daily or hourly basis. As illustrated in Fig. 7, the two winds are represented by pink and black arrows, respectively. There is a negligible difference between the two days. This map facilitates the evaluation of wind direction and magnitude along the shoreline, and Table 3 summarizes those parameters: the wind has a direction of around 276° and an intensity between 2.5 and 4.8 m/s. At the eastern beach (KB), the wind blows toward the shore, potentially moving MPs released into the environment from Lombok Island and keeping those emitted by local sources in place. Conversely, on the beaches located on the western side of the island of Bali, the wind blows toward the sea, thus potentially carrying potential MPs emitted by sources of impact located behind them, on the mainland, to the beaches. Wind on the day of sampling ranged from a maximum of 5–7 m/s.

Another parameter that has been considered is wind waves, as illustrated in Fig. 8, which summarizes its three descriptive parameters: direction, wave height, and period. The direction is expressed in degrees from the point of origin. The area in proximity to KB exhibited negligible wave motion, with the satellite-measured height recorded as 0 m and the wave period also reported as minimal. This suggests that the sea conditions in the immediate period prior to sampling were of a very calm nature. In contrast, the wave motion exhibited greater consistency in BB and NNB, despite the heights being less than 1 m and the period measuring approximately 2 s (s).

The integrated interpretation of current, wind, and wind wave data (Table 3, Figs. 6–8) provides qualitative insight into the hydrodynamic processes that may contribute to the accumulation of MPs along the beaches studied. These data suggest possible retention and dispersion events at each sampling site, which may contribute to the observed variability in MP concentrations.

At KB, the observed ocean current direction (~240°) and relatively high intensity (~1.1 m/s) are consistent with the seasonal circulation associated with the Lombok Strait. During the sampling period, the wind (~277°, ~2.6 m/s) was directed toward the coast, while wave conditions were characterized by short periods (1.2 s) and variable directions (20–250°). This hydrodynamic configuration may favor the nearshore retention of floating debris, particularly under conditions of limited offshore transport. Accordingly, the relatively higher MP concentrations observed at KB (2.54 ± 2.30 MPs/kg dw) could reflect a retention-prone setting in which onshore wind stress and persistent currents promote accumulation in the surf and breaking zones.

At BB, surface currents were weaker (~0.31 m/s) and oriented southward (~187°), while winds were stronger (~4.8 m/s) and directed offshore (~277°). Waves approached from 126°, with moderate periods (1.8 s) and heights (0.34 m). The combined influence of weaker currents and offshore-directed winds may enhance dispersion and resuspension of floating particles, facilitating their export away from the shoreline. This hydrodynamic setting could contribute to reduced MP retention on

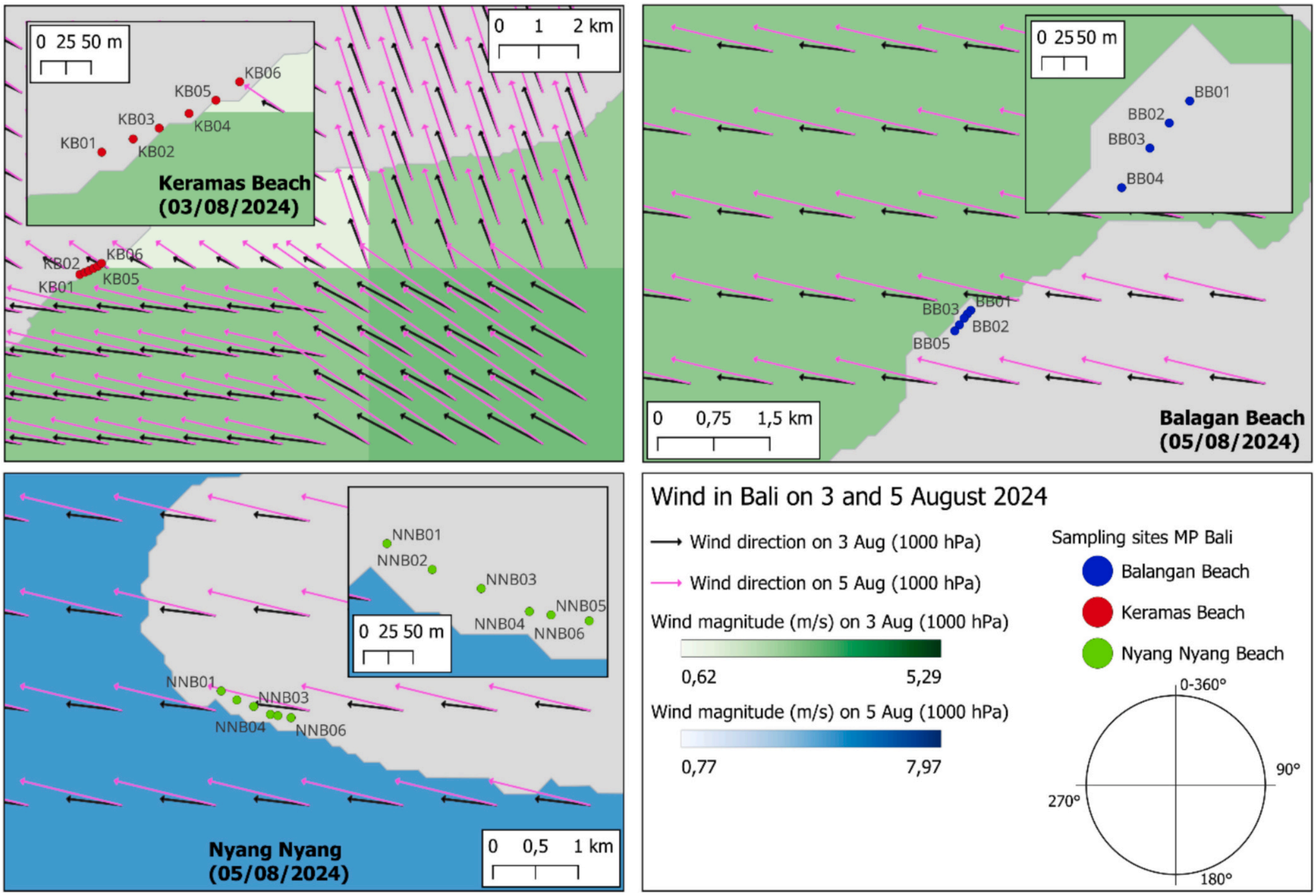

Fig. 7. Winds at 1000 hPa on 3 and 5 of August 2024 on the individual beaches. Detailed sampling sites are highlighted, and wind direction and magnitude (as arrow length) are represented for 3 and 5 August 2024 as the 12:00 hourly average. Magnitude is also represented in scaled colors: greens for 3 August and blues for 5 August. Note that for wind, direction in degrees indicates where the wind is headed. Wind data are derived from CAMS Global atmospheric composition forecasts (CAMS, 2024b), with a satellite resolution of approximately 40 km, the wind speed RMSE is 1–3 m/s.

the beach surface, consistent with the lower MP abundance measured at BB (0.61 ± 1.37 MPs/kg dw).

At NNB, the dominant wave and current directions (~126° and ~183°, respectively) were approximately parallel to the coastline, while wind conditions (~277°, ~4.8 m/s) imposed oblique forcing under relatively low wave energy (h ≈ 0.21 m; t ≈ 2 s). These conditions may promote the development of a weak but persistent longshore drift (~0.27 m/s), favoring lateral redistribution of floating material along the shoreline rather than strong cross-shore transport. Such a regime could explain the intermediate MP concentrations observed at NNB (2.04 ± 2.49 MPs/kg dw), potentially reflecting localized zones of accumulation along the beach.

Overall, the comparison among the three beaches suggests that MP retention may be influenced by the balance between current intensity, wind stress, and wave energy, with onshore-directed forcing favoring accumulation and offshore-directed components enhancing dispersion. Under this framework, KB may function as a convergence-prone environment, BB may represent a more dispersive coastal setting, and NNB may exhibit transitional behavior characterized by alongshore redistribution.

In addition to hydrodynamic controls, spatial variability in MP abundance is likely also modulated by anthropogenic pressures. KB is located in a highly touristic area and is bordered by multiple small rivers and drainage channels, which may increase local MP inputs through urban runoff and recreational activities. NNB experiences lower direct urban influence; however, intermediate MP levels could be associated with regional transport from riverine sources along northern Bali, where several moderate to high plastic discharge rivers have been identified (Meijer et al., 2021b). The prevailing southward coastal currents may facilitate the redistribution of river-derived plastics along the western coastline. BB, situated along a less developed coast with limited local sources, exhibited the presence of PS fragments, which may indicate external inputs, potentially linked to fishing activities, shipping routes, or episodic long-range transport from Java during seasonal current reversals.

3.3. Policy and management implications

Indonesia continues to experience substantial challenges in managing plastic waste, despite the presence of national and regional policy frameworks. The country generates an estimated 64 million tonnes of plastic waste annually and remains one of the largest global contributors to marine plastic pollution (Idris et al., 2024). Bali, which relies heavily on tourism and coastal-based economic activities, is particularly impacted due to high waste generation and intensified consumption patterns (MacRae, 2012). The National Waste Management Policy and Strategy (2017) outlined targets to reduce waste generation by 30% and ensure that 70% of waste is properly managed by 2025 (Sumaryana et al., 2025). However, progress toward these goals has been uneven, primarily due to weak institutional coordination, insufficient infrastructure, and limited regulatory enforcement (Subekti, 2023; Apriadi et al., 2024).

At the provincial level, Bali has implemented several notable policy measures, including the prohibition of plastic bags, drinking straws, and

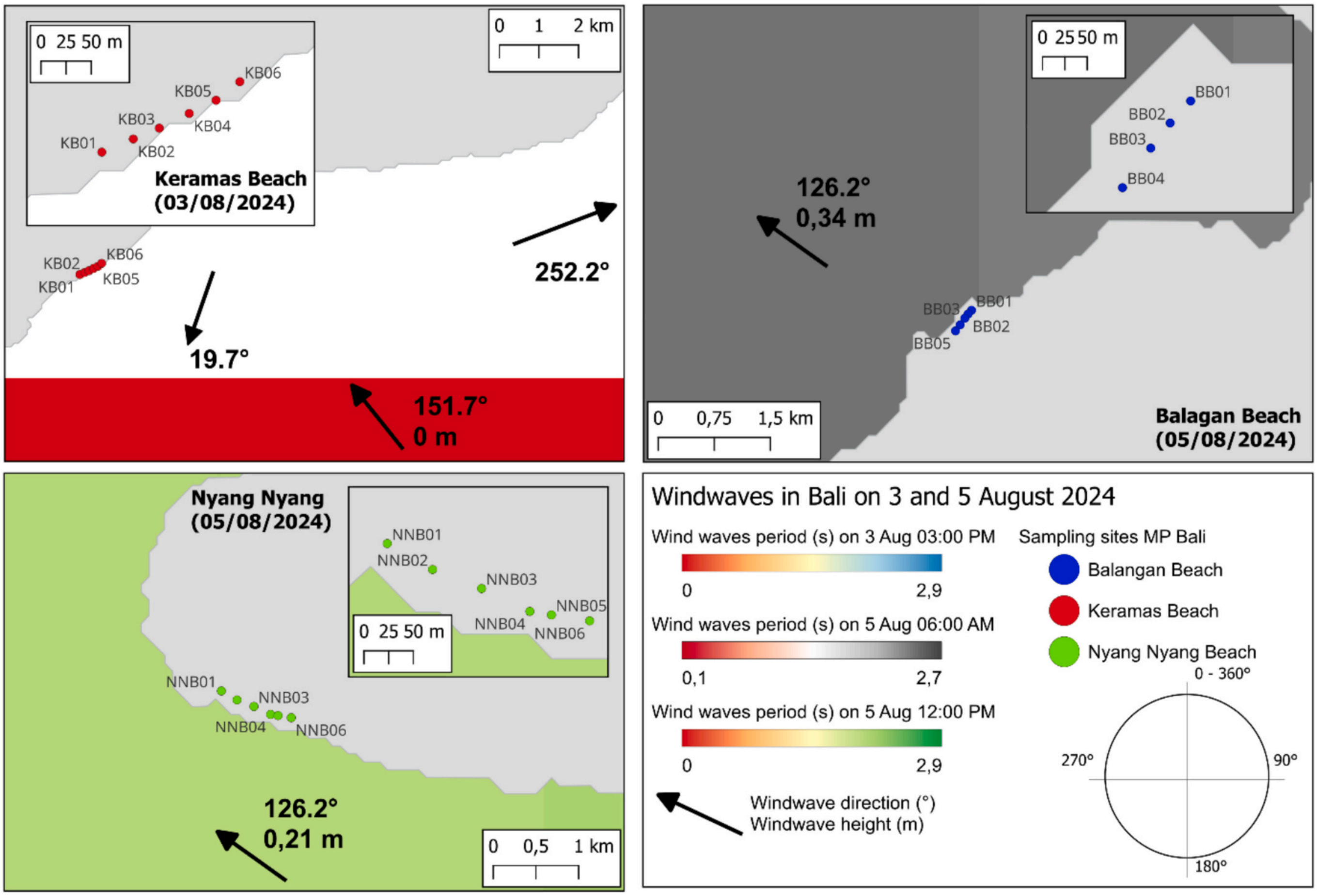

Fig. 8. Wind waves on 3 and 5 August 2024 on the individual beaches. Detailed sampling sites are highlighted, and wind waves direction, magnitude, and height are represented for 3 and 5 August 2024. The color-based layer represents the period, and arrows indicate the direction. Note that for waves, direction in degrees indicates where the wave is coming from. Wind waves data comes from the Global Ocean Waves Analysis and Forecast by CMEMS (CMEMS, 2024b), that has a spatial resolution of 1/12° (~0.083°), corresponding to approximately 8 km, temporal averaging is 3 h, and uncertainty declared by CMES on significant wave height is Global average of bias: 2 cm and Global average of normalized scatter index: 13.8%.

Styrofoam products, supported by community-based waste management initiatives involving government authorities, non-governmental organizations, and local businesses (Sumaryana et al., 2025). Despite these interventions, challenges remain in sustaining compliance and ensuring continuous monitoring and evaluation. Limited accountability mechanisms and gaps in enforcement reduce the long-term effectiveness of these policies (Ain et al., 2021).

Therefore, future strategies should emphasize active community participation and educational engagement. Integrating environmental awareness programmes at the school and community levels, and involving both local residents and foreign visitors in waste monitoring activities, could help increase public understanding of MP pollution in coastal areas. In addition, regular river and beach clean-up initiatives, specifically targeting the removal of synthetic polymer residues, could be strengthened through partnerships with tourism industry stakeholders and corporate sponsors. Sustained collaboration and shared responsibility among governmental bodies, the private sector, and local communities are essential to achieving substantial and long-lasting improvements in plastic waste management across Bali and Indonesia.

Future work may also benefit from developing a more comprehensive mathematical model that combines satellite-derived hydrodynamic information, such as currents, wind patterns, and wave conditions, with field-based measurements of MP concentrations on beaches. Integrating these datasets would allow more realistic simulations of MP transport and deposition, improving our ability to predict where accumulation is likely to occur. Such a model could also provide useful guidance for management efforts by helping identify priority areas for mitigation and targeted beach clean-up activities.

4. Conclusion

This study provides an integrated spectroscopic–oceanographic assessment of MP contamination across three beaches in Bali between January and July 2024, combining ATR-FTIR polymer characterization with satellite-derived hydrodynamic data from CMEMS and CAMS. Within the sampling period, the abundance of MPs in the beach sediments was relatively low (<10 MPs/kg dw), yet clear spatial patterns emerged. KB exhibited the highest MP concentration (2.54 ± 2.30 MPs/kg dw), followed by NNB (2.04 ± 2.49 MPs/kg dw), while BB showed the lowest levels (0.61 ± 1.37 MPs/kg dw). FTIR analysis revealed PS as the dominant polymer, followed by PP, PVA, PMMA, and three other copolymers. Fragments were the most abundant form, and particles in the 2.5–5 mm size class predominated. The correspondence between the sampled MPs and reference library spectra, reflected by characteristic IR absorption bands, indicates that ATR-FTIR can be used for polymer identification in complex coastal matrices, within the limitations of spectral quality and sample heterogeneity. The spatial heterogeneity of MP distribution was strongly governed by seasonal variability in ocean currents, wind fields, and wind wave energy. Hydrodynamic patterns indicated that KB experienced aligned onshore winds and moderately strong southwestward currents originating from the Lombok Strait, promoting MP retention and deposition. In contrast, BB was influenced by weaker currents and strong offshore winds, creating a dispersive environment unfavorable for MP accumulation. NNB received oblique winds and longshore currents that redistributed particles laterally, producing intermediate MP concentrations. These findings underscore the importance of coastal hydrodynamics as drivers of MP transport, retention, and export at fine spatial scales, while also reflecting the influence of local anthropogenic pressures, including riverine discharge, tourism activity, and shoreline infrastructure. Overall, this work highlights that even beaches with relatively low MP loads can exhibit distinct contamination signatures shaped by the interplay of polymer sources, coastal morphology, and seasonal oceanographic processes. By integrating physical oceanographic data with MP distribution, the study provides a more mechanistic understanding of MP transport pathways in the coastal system of Bali. This combined approach strengthens the foundation for future predictive modeling efforts and supports the design of targeted mitigation strategies. Incorporating hydrodynamic simulations with expanded temporal sampling and higher-resolution riverine input data will be crucial for forecasting MP accumulation hotspots and informing policy interventions aimed at reducing plastic pollution in the coastal environments of Indonesia.

Beyond these scientific insights, the study outcomes hold practical relevance for regional management. The GIS-based mapping framework is a tool that local environmental authorities can use to manage and monitor target areas. This framework facilitates the prioritization of sampling and cleanup efforts at beaches that are particularly affected by convergent current systems, such as KB and NNB. The seasonal current reversals identified through satellite analysis are a great opportunity to adjust waste management strategies seasonally, with intensified shoreline cleanup and waste interception at river mouths prior to the onset of the northwest monsoon, when eastward transport from Java is dominant. From a policy perspective, integrating remote sensing tools with routine beach surveys has the potential to establish a cost-effective, semi-automated early warning system for plastic accumulation zones around Bali. Such a system could be progressively developed by repeating studies like this one several times throughout the year and systematically combining MP monitoring with satellite observations. These findings provide essential baseline information to support evidence-based pollution management strategies aimed at Bali.

4.1. *Limitations and future work*

The detection capability of the present study is constrained by the minimum sieve mesh size of 212 μm; consequently, MPs smaller than this threshold were not captured or reported. This limitation reflects methodological constraints rather than the absence of smaller MPs in the environment, and the results should therefore be interpreted as representative only of the larger MP size fraction.

A major methodological limitation is the absence of field blanks and explicit airborne contamination controls. Given the relatively low number of particles recovered ($n = 44$), potential contamination during field sampling, sample handling, and laboratory processing cannot be fully excluded. Such contamination may influence reported particle counts, size distributions, and polymer identification, particularly for small fragments. Accordingly, the reported MP abundances should be regarded as conservative estimates rather than absolute concentrations.

The density separation procedure relied exclusively on seawater, introducing a systematic bias toward the recovery of low-density polymers. Higher-density polymers are therefore likely underrepresented, and observed polymer dominance patterns may not accurately reflect true environmental proportions. Consequently, conclusions regarding polymer composition and relative abundance should be interpreted with caution and framed as baseline or exploratory observations.

Additional constraints arise from the limited sample size and sampling strategy, which restrict the dataset's representativeness and limit broader spatial generalization across beaches in Bali. Polymer identification relied on existing spectral libraries, which may not fully capture the spectral variability of weathered or environmentally aged MPs, potentially leading to ambiguous or conservative classifications. Furthermore, the hydrodynamic analysis is based on satellite-derived products with relatively coarse spatial resolution in nearshore environments, which may reduce the accuracy of current and wind estimates close to the coastline. Although satellite observations provide the most spatially consistent datasets available for the region, the lack of extensive in situ validation data constrains full calibration and verification of MP transport interpretations. Consequently, the mechanistic relationships inferred between hydrodynamic drivers and MP deposition should be regarded as plausible but provisional hypotheses requiring further experimental or inferential validation.

Taken together, the relatively low confirmed MP concentrations (0.61 ± 1.37 to 2.54 ± 2.30 MPs/kg dw) across a broad spatial scale limit statistical robustness and reduce the ability to detect subtle spatial gradients or confidently generalize observed patterns. Variability estimates and mean concentrations are therefore sensitive to individual particle detections, increasing uncertainty in abundance metrics and polymer distribution patterns. As a result, the findings should be interpreted as indicative of relative spatial trends and hydrodynamic influences rather than definitive or comprehensive assessments of MP contamination along Bali's coastline.

Future studies should address these limitations by incorporating procedural, field, and airborne blanks to minimise contamination-related uncertainty; adopting higher density separation solutions (e.g., $CaCl_2$ or NaCl) to improve recovery of denser polymers; and employing finer mesh sizes to capture smaller MP fractions, including pathways toward nanoplastic investigation. Expanding sample numbers and spatial coverage will enhance statistical robustness, improve representativeness, and allow more reliable spatial comparisons.

Polymer identification of smaller than the current limit can be strengthened by integrating complementary analytical techniques such as optical photothermal infrared (OPTIR) spectroscopy, Raman spectroscopy, and pyrolysis-GC/MS, particularly for weathered, mixed, or ambiguous particles. The development and use of spectral libraries that explicitly include environmentally aged MPs would further enhance classification accuracy and confidence in polymer assignments.

To improve understanding of MP transport processes, future research should prioritize in situ validation of satellite-derived hydrodynamic products, addressing a key limitation of remote-sensing-based MP studies. Building on this, the development of a robust mathematical model integrating satellite-derived hydrodynamic data with field-based MP measurements would provide a quantitative framework for simulating MP transport, accumulation, and fate. Such a model could improve predictive capability, identify accumulation hotspots, and serve as a valuable decision-support tool for targeted MP management and mitigation strategies in coastal environments.

CRediT authorship contribution statement

Mohd Rashidi Abdull Manap: Writing – review & editing, Writing – original draft, Visualization, Validation, Supervision, Software, Resources, Project administration, Methodology, Investigation, Funding acquisition, Formal analysis, Data curation, Conceptualization. **Muhammad Ibadurrahman bin Imizan:** Writing – review & editing, Writing – original draft, Visualization, Software, Resources, Methodology, Investigation, Formal analysis, Data curation, Conceptualization. **Jannik Werner Dams:** Writing – review & editing, Writing – original draft, Visualization, Validation, Software, Resources, Project administration, Methodology, Investigation, Formal analysis, Data curation, Conceptualization. **Felipe D. Sepulveda:** Writing – review & editing, Writing – original draft, Visualization, Validation, Supervision, Software, Resources, Methodology, Investigation, Formal analysis, Data curation, Conceptualization. **Anna Muratore:** Writing – review & editing, Writing – original draft, Visualization, Validation, Software, Resources, Methodology, Investigation, Formal analysis, Data curation.

Lorenza Notargiacomo: Writing – review & editing, Writing – original draft, Visualization, Validation, Software, Resources, Methodology, Investigation, Formal analysis, Data curation. **Fulvio Ferrara:** Writing – review & editing, Writing – original draft, Visualization, Validation, Supervision, Software, Resources, Project administration, Methodology, Investigation, Formal analysis, Data curation, Conceptualization. **Nur Hayatna Mukhni:** Writing – review & editing, Writing – original draft, Formal analysis, Data curation, Conceptualization, Investigation, Validation, Visualization.

Funding

Supported by Geran Putra-Inisiatif Putra Muda (GP-IPM/2023/9741500) and GP-Fast Track/2024/9791800.

Declaration of competing interest

The authors declare no competing interests.

Acknowledgements

The authors extend their gratitude to Kyushu University, Japan, for their instrumental support in collecting ATR-FTIR spectra. We also appreciate the presence and contributions of two students, Muhammad Ibadurrahman bin Imizan and Jannik Dams Werner, from the University of Manchester and the University of Bonn, respectively, for their excellent fieldwork in sampling collection in their capacity as interns as part of the UPM Inbound Mobility Programme. Also, Ramizah Azis (IKTBN Sepang, Selangor), Abu Rayyan Mohd Rashidi (SMK Seri Serdang, Selangor), and Rayna Mohd Rashidi (SK Serdang, Selangor) are acknowledged for their contributions to the logistics process in Bali.

Appendix A. Supplementary data

Supplementary data to this article can be found online at https://doi.org/10.1016/j.jconhyd.2026.104864.

Data availability

The datasets analyzed in this study are publicly available on Mendeley Data:•

Microscopic images: https://data.mendeley.com/datasets/58fgc8xmdw/1.•

FTIR spectra: https://data.mendeley.com/datasets/h9d5mkbvzn/1.•

Geospatial mapping of sampling sites: https://data.mendeley.com/datasets/4398vvvvzj/1.

References

Adhinugraha, F.A.C., Atmadipoera, A.S., Hartanto, M.T., 2023. The ocean response to El Nino southern oscillation (ENSO) in the Bali Sea: a model study. IOP Conf. Ser. Earth Environ. Sci. https://doi.org/10.1088/1755-1315/1137/1/012014.

Ain, K.Q., Nasri, M.A., Alamsyah, M.N., Pratama, M.D.R., Kurniawan, T., 2021. Collaborative governance in managing plastic waste in Bali. IOP Conf. Ser. Earth Environ. Sci. 905, 012115. https://doi.org/10.1088/1755-1315/905/1/012115.

Ajay, K., Kumar, S., Kaushal, S., Resmi, M.R., Singh, A., Anoop, A., 2025. Source-to-sink dynamics of microplastics and heavy metals along a land-use gradient in the tropical river system of India. J. Hazard. Mater. Adv. 20, 100899. https://doi.org/10.1016/j.hazadv.2025.100899.

Alkoiri, M.F., Ramdhan, M., Setyamarta, G., Hayati, N., 2024. Estimation of potential skipjack tuna fishing ground using MODIS data in 2020–2021 (case study: Bali Strait). Springer Proc. Phys. 341–352. https://doi.org/10.1007/978-981-97-0740-9_31.

Aouissi, T., Baouz, T., Hellati, A., Zerriouh, A., Benaniba, M.T., Benachour, D., Hasan, M., Benguerba, Y., 2023. Enhancing compatibility and properties of polylactic acid/polystyrene (PLA/PS) bioblend for sustainable food packaging: experimental and quantum computational insights. Mater. Today Commun. 37. https://doi.org/10.1016/j.mtcomm.2023.107106.

Apriadi, B.F., Setiawan, R.P., Firmansyah, I., 2024. Policy scenario of plastic waste mitigation in Indonesia using system dynamics. Waste Manag. Res. 42, 1008–1018. https://doi.org/10.1177/0734242X241231396.

Asadi, M.A., Ritonga, Y.A.P., Yona, D., Hertika, A.M.S., 2019. Vertical distribution of microplastics in coastal sediments of Bama resort, Baluran National Park, Indonesia. Nat. Environ. Pollut. Technol. 18, 1169–1176.

Borah, A., Hande, O.M., Jayakumar, S., Devipriya, S.P., 2024. Microplastic pollution in beach sediments in the Dapoli coast, Maharashtra, the western peninsular region of India. Reg. Stud. Mar. Sci. 77. https://doi.org/10.1016/j.rsma.2024.103640.

Bridson, J.H., Patel, M., Lewis, A., Gaw, S., Parker, K., 2020. Microplastic contamination in Auckland (New Zealand) beach sediments. Mar. Pollut. Bull. 151. https://doi.org/10.1016/j.marpolbul.2019.110867.

Cai, C., Zhu, L., Hong, B., 2023. A review of methods for modeling microplastic transport in the marine environments. Mar. Pollut. Bull. 193. https://doi.org/10.1016/j.marpolbul.2023.115136.

CAMS, 2024a. Global Greenhouse Gas Forecasts [WWW Document]. Copernicus Atmosphere Monitoring Service (CAMS). https://doi.org/10.24381/93910310.

CAMS, 2024b. Global Atmospheric Composition Forecasts [WWW Document]. Copernicus Atmosphere Monitoring Service (CAMS). https://doi.org/10.24381/04a0b097.

Carvalho, A.B., Farias, C.N., de Castro Vasconcellos, P., Fernandes, A.N., de Sales, F., Chiquetto, J.B., de Lima, N.G.B., Baratto, J., Gobo, J.P.A., 2025. Detection, characteristics, and some influencing factors of MPs in rainfall. Theor. Appl. Climatol. 156. https://doi.org/10.1007/s00704-025-05441-y.

Chairunnisa, N.K., Adam, Moh A., Candri, D.A., 2025. Microplastic pollution in the aquatic ecosystem of Gili Trawangan, Lombok: abundance, characteristics, and implications in tourism area. Jurnal Penelitian Pendidikan IPA 11, 907–916. https://doi.org/10.29303/jppipa.v11i7.7485.

CMEMS, 2024a. Global Ocean Physics Analysis and Forecast [WWW Document]. Copernicus Marine Environment Monitoring Service (CMEMS). https://doi.org/10.48670/moi-00016.

CMEMS, 2024b. Global Ocean Waves Analysis and Forecast [WWW Document]. Copernicus Marine Environment Monitoring Service (CMEMS). https://doi.org/10.48670/moi-00017.

Curren, E., Yew Leong, S.C., 2023. Spatiotemporal characterisation of microplastics in the coastal regions of Singapore. Heliyon 9, e12961. https://doi.org/10.1016/j.heliyon.2023.e12961.

Dohan, K., Maximenko, N., 2010. Monitoring ocean currents with satellite sensors. Oceanography 23, 94–103.

Gimiliani, G.T., Fornari, M., Redígolo, M.M., Willian Vega Bustillos, J.O., Moledo de Souza Abessa, D., Faustino Pires, M.A., 2020. Simple and cost-effective method for microplastic quantification in estuarine sediment: a case study of the Santos and São Vicente estuarine system. Case Stud. Chem. Environ. Eng. 2, 100020. https://doi.org/10.1016/j.cscee.2020.100020.

Hee, Y.Y., Hanif, N.M., Weston, K., Latif, M.T., Suratman, S., Rusli, M.U., Mayes, A.G., 2023. Atmospheric microplastic transport and deposition to urban and pristine tropical locations in Southeast Asia. Sci. Total Environ. 902. https://doi.org/10.1016/j.scitotenv.2023.166153.

Ho, C.M., Feng, W., Li, X., Ngien, S.K., Yu, X., Song, F., Yang, F., Liao, H., 2025. Microplastic distribution and its implications for human health through marine environments. J. Environ. Manag. 382. https://doi.org/10.1016/j.jenvman.2025.125427.

Idris, S.H., Puteri, D.S., Wahono, D.C., Firdaus, Rr J., Pratomo, N.B.A., 2024. Indonesia paradox on plastic waste import in international policy and social movement perspective. Indonesian J. Advoc. Legal Serv. 6, 169–204. https://doi.org/10.15294/ijals.v6i1.78522.

Iskandar, M.R., Park, Y.-G., Surinati, D., Nugroho, D., Cordova, M.R., 2024. Estimation of bottom microplastic flux in the Indonesian seas. Mar. Pollut. Bull. 209. https://doi.org/10.1016/j.marpolbul.2024.117047.

Jiang, J., He, L., Zheng, S., Liu, J., Gong, L., 2024. A review of microplastic transport in coastal zones. Mar. Environ. Res. 196, 106397. https://doi.org/10.1016/J.MARENVRES.2024.106397.

Kannankai, M.P., Devipriya, S.P., 2024. Atmospheric microplastic deposition in a coastal city of India: the influence of a landfill source on monsoon winds. Sci. Total Environ. 908. https://doi.org/10.1016/j.scitotenv.2023.168235.

Karimi, M., Markazi, S.A., Javanmardi, M., Teshnizi, M.S., Khoramshahi, H., Avakh, Z., 2024. Artificial intelligence and machine learning approaches for automatic microplastics identification and characterization. In: Fate of Microplastics in Wastewater Treatment Plants: Occurrence, Identification, Potential Factors, and Future Perspectives, pp. 187–206. https://doi.org/10.1201/9781003438793-14.

Kumar, S., Behera, D., Ajay, K., Karthick, B., Dharia, C., Anoop, A., 2024. Microplastics and heavy metal contamination along a land-use gradient in a Himalayan foothill river: prevalence and controlling factors. J. Contam. Hydrol. 266, 104411. https://doi.org/10.1016/j.jconhyd.2024.104411.

Kumar, S., Ajay, K., Behera, D., Yaseen, A., Karthick, B., Prasad, S., Bhat, S.U., Jehangir, A., Anoop, A., 2025. Co-occurrence of microplastics and heavy metals in a freshwater lake system in Indian Himalaya: distribution and influencing factors. Emerg. Contam. 11, 100394. https://doi.org/10.1016/j.emcon.2024.100394.

Li, J., Gao, F., Zhang, D., Cao, W., Zhao, C., 2022. Zonal distribution characteristics of microplastics in the southern Indian Ocean and the influence of ocean current. J. Mar. Sci. Eng. 10. https://doi.org/10.3390/jmse10020290.

Ma, J., Ma, R., Pan, Q., Liang, X., Wang, J., Ni, X., 2023. A global review of progress in remote sensing and monitoring of marine pollution. Water (Switzerland) 15. https://doi.org/10.3390/w15193491.

MacRae, G., 2012. Solid waste management in tropical Asia: what can we learn from Bali? Waste Manag. Res. 30, 72–79. https://doi.org/10.1177/0734242X10386138.

Mali, D.D., Nivrutti, S.S., Gadekar, M.J., 2025. Application of artificial intelligence to improve microplastic identification. In: Microplastics Pollution Control in Water Systems: Practical Solutions, pp. 169–187. https://doi.org/10.1007/978-3-031-74399-3_8.

Manap, M.R.A., 2024a. Image of Particles from Marine Sediment Samples Collected in Bali and Aceh in August at UPM, Malaysia [WWW Document]. Mendeley Data. URL. https://data.mendeley.com/datasets/58fgc8xmdw/1.

Manap, M.R.A., 2024b. Infrared of Particles from Marine Sediment Samples Collected in Bali Island in August 2024 using a Shimadzu Spectrometer at COPS-Thailand, Kyushu University [WWW Document]. Mendeley Data. URL. https://data.mendeley.com/datasets/h9d5mkbvzn/1.

Manap, M.R.A., 2025. Geospatial Mapping of Sampling Sites in Bali and Banda Aceh Using KML Format [WWW Document]. Mendeley Data. URL. https://data.mendeley.com/datasets/4398vvvvzj/1.

Manullang, C.Y., Patria, M.P., Haryono, A., Anuar, S.T., Fadli, M., Susanto, R.D., Wei, Z., 2024. Vertical distribution of microplastic along the main gate of Indonesian Throughflow pathways. Mar. Pollut. Bull. 199. https://doi.org/10.1016/j.marpolbul.2023.115954.

Mauludy, M.S., Yunanto, A., Yona, D., 2019. Microplastic abundances in the sediment of coastal beaches in Badung, Bali. Jurnal Perikanan Universitas Gadjah Mada 21, 73. https://doi.org/10.22146/jfs.45871.

Meijer, L.J.J., van Emmerik, T., van der Ent, R., Schmidt, C., Lebreton, L., 2021a. More than 1000 rivers account for 80% of global riverine plastic emissions into the ocean. Sci. Adv. 7. https://doi.org/10.1126/sciadv.aaz5803.

Meijer, L.J.J., van Emmerik, T., van der Ent, R., Schmidt, C., Lebreton, L., 2021b. Supplementary Data for "More Than 1000 Rivers Account for 80% of Global Riverine Plastic Emissions into the Ocean" [WWW Document]. URL. https://figshare.com/articles/dataset/Supplementary_data_for_More_than_1000_rivers_account_for_80_of_global_riverine_plsatic_emissions_into_the_ocean_/14515590?file=27807774 (accessed 1.9.25).

Nakano, H., Alfonso, M.B., Phinchan, N., Jandang, S., Manap, M.R.A., Chavanich, S., Viyakarn, V., Müller, M., Wong, C., Bacosa, H.P., Celik, M., Cordova, M.R., Isobe, A., 2025. Aquatic microplastics research in the ASEAN region: analysis of challenges and priorities. Mar. Pollut. Bull. 210, 117342. https://doi.org/10.1016/j.marpolbul.2024.117342.

Noor, S.Y., Riani, E., Hariyadi, S., Butet, N.A., Cordova, M.R., 2025. Characterisation and abundance of microplastic pollution in sediments of Banten Bay, Indonesia. Chem. Ecol. 41, 823–842. https://doi.org/10.1080/02757540.2025.2498155.

Prajapati, A., Jadhao, P., Kumar, A.R., 2025. Atmospheric microplastics deposition in a central Indian city: distribution, characteristics and seasonal variations. Environ. Pollut. 374. https://doi.org/10.1016/j.envpol.2025.126183.

Raja, K.J., Buijsman, M.C., Bozec, A., Helber, R.W., Shriver, J.F., Wallcraft, A., Chassignet, E.P., Arbic, B.K., 2024. Spurious internal wave generation during data assimilation in eddy resolving ocean model simulations. Ocean Model (Oxf.) 188. https://doi.org/10.1016/j.ocemod.2024.102340.

Rathore, C., Saha, M., Gupta, P., Kumar, M., Naik, A., de Boer, J., 2023. Standardization of micro-FTIR methods and applicability for the detection and identification of microplastics in environmental matrices. Sci. Total Environ. 888. https://doi.org/10.1016/j.scitotenv.2023.164157.

Riani, E., Cordova, M.R., 2022. Microplastic ingestion by the sandfish *Holothuria scabra* in Lampung and Sumbawa, Indonesia. Mar. Pollut. Bull. 175. https://doi.org/10.1016/j.marpolbul.2021.113134.

Subekti, R., 2023. A circular economy-based plastic waste management policy in Indonesia (compared to China and EU). Yustisia Jurnal Hukum 12, 168. https://doi.org/10.20961/yustisia.v12i2.72177.

Sumaryana, A., Komara, S.R., Pancasilawan, R., 2025. Organizational capacity in implementing the "Kang Pisman" program: a case study of waste management in Bandung City. J. Ecohumanism 4. https://doi.org/10.62754/joe.v4i1.6011.

Suntoyo, O.P.K.R., Wahyudi, 2021. Water quality modeling distribution at Bali Strait in the Western monsoon and its impact for ecosystems. IOP Conf. Ser. Earth Environ. Sci. https://doi.org/10.1088/1755-1315/698/1/012023.

Suteja, Y., Purwiyanto, A.I.S., Purbonegoro, T., Cordova, M.R., 2024. Spatial and temporal trends of microplastic contamination in surface sediment of Benoa Bay: an urban estuary in Bali-Indonesia. Mar. Pollut. Bull. 202, 116357. https://doi.org/10.1016/j.marpolbul.2024.116357.

Takarina, N.D., Purwiyanto, A.I.S., Rasud, A.A., Arifin, A.A., Suteja, Y., 2022. Microplastic abundance and distribution in surface water and sediment collected from the coastal area. Glob. J. Environ. Sci. Manag. 8, 183–196. https://doi.org/10.22034/GJESM.2022.02.03.

TheOceanCleanup, 2017. River Plastic Pollution Sources | The Ocean Cleanup [WWW Document]. URL. https://theoceancleanup.com/sources/ (accessed 1.9.25).

Thibault, M., Fajeau, A., Ramanampananjy, A., Royer, S.-J., Fustemberg, G., Marillac, V., Gindrey, J., Saloma, A., Condet, M., Mangion, P., Burt, A., Egger, M., Amy, M., Jaquemet, S., Mulochau, T., Jourand, P., Ter Halle, A., Le Corre, M., Lebreton, L., 2025. Concentration gradient of plastic debris larger than 500 μm detected across the southwest Indian ocean. Sci. Rep. 15, 22364. https://doi.org/10.1038/s41598-025-02893-0.

Tjahjono, A., Cahyadi, T., Wibisono, Y., Sugiharto, R., Wahyuni, O., 2024. The relevance of microplastics (MPs) abundance and trace metal Pb at the estuaries of ECF and Babon River, Semarang, Indonesia. Egypt. J. Aquat. Res. 50, 301–308. https://doi.org/10.1016/j.ejar.2024.05.001.

Wang, X., Liu, K., Zhu, L., Li, C., Song, Z., Li, D., 2021. Efficient transport of atmospheric microplastics onto the continent via the East Asian summer monsoon. J. Hazard. Mater. 414. https://doi.org/10.1016/j.jhazmat.2021.125477.

Widyananto, P.A., Badriana, M.R., Oktaviani, D.F., Radjawane, I.M., 2024. Preliminary study of marine environmental parameters in the southeastern coastal area of Bali, Indonesia. IOP Conf. Ser. Earth Environ. Sci. https://doi.org/10.1088/1755-1315/1410/1/012050.

Wijaya, A., Zakiyah, U., Sambah, A.B., Setyohadi, D., 2020. Spatio-temporal variability of temperature and chlorophyll-a concentration of sea surface in Bali strait, Indonesia. Biodiversitas 21, 5283–5290. https://doi.org/10.13057/biodiv/d211132.

Yang, X., Li, X., Pichel, W.G., Li, Z., 2011. Comparison of ocean surface winds from ENVISAT ASAR, MetOp ASCAT scatterometer, buoy measurements, and NOGAPS model. IEEE Trans. Geosci. Remote Sens. 49, 4743–4750. https://doi.org/10.1109/TGRS.2011.2159802.

Yona, D., Setyawan, F.O., Putri, S.E.N., Iranawati, F., Kautsar, M.A., Isobe, A., 2023. Microplastic distribution in beach sediments: comparison between the north and south waters of East Java Island, Indonesia. Jurnal Ilmiah Perikanan Dan Kelautan 15, 303–315. https://doi.org/10.20473/jipk.v15i2.41065.

Zahari, N.Z., Vincent, S.D., Cleophas, F.N., Budin, K., Sabullah, M.K., 2023. Abundance, distribution, and characterization of microplastics on two recreational beaches in Kota Kinabalu, Sabah, Malaysia. Water (Basel) 15, 2681. https://doi.org/10.3390/w15152681.